

Random diffusivity scenarios behind anomalous non-Gaussian diffusion

M. A. F. dos Santos¹, E. H. Colombo^{2,3} and C. Anteneodo^{1,4}

¹ *Department of Physics, PUC-Rio, Rua Marquês de São Vicente 225,
22451-900, Rio de Janeiro, RJ, Brazil*

² *Department of Ecology & Evolutionary Biology,
Princeton University, Princeton, NJ 08544, USA*

³ *Department of Ecology, Evolution,
and Natural Resources,*

Rutgers University, New Brunswick, NJ 08901, USA and

⁴ *Institute of Science and Technology for Complex Systems, Brazil*

Abstract

The standard diffusive spreading, characterized by a Gaussian distribution with mean square displacement that grows linearly with time, can break down, for instance, under the presence of correlations and heterogeneity. In this work, we consider the spread of a population of fractional (long-time correlated) Brownian walkers, with time-dependent and heterogeneous diffusivity. We aim to obtain the possible scenarios related to these individual-level features from the observation of the temporal evolution of the population spatial distribution. We develop and discuss the possibility and limitations of this connection for the broad class of self-similar diffusion processes. Our results are presented in terms of a general framework, which is then used to address well-known processes, such as Laplace diffusion, nonlinear diffusion, and their extensions.

Keywords: Superstatistics; Anomalous diffusion; Fractional Brownian motion; Scaled diffusion

I. INTRODUCTION

Diffusion processes are a fundamental ingredient of the dynamics of spatially-extended physical, chemical and biological systems. Regardless of the entity, from nanoparticles to complex biological organisms, it is common that, due to the lack of coherence in external drivers, random, uncorrelated motion can arise. In the case of Brownian motion (Bm), the spreading of a given substance follows normal diffusion, characterized by (i) a Gaussian distribution, (ii) with mean square displacement (MSD) that grows linearly with time.

These two remarkable properties are quite ubiquitous in nature, but tend to break down under more complex scenarios. For instance, a class of situations produce the so-called Brownian yet non-Gaussian behavior, which implies a deviation from the Gaussian shape, but preserving the linear law of the MSD [1]. In contrast, in other cases, the Gaussian shape can be preserved, while the mean square displacement, $\langle \mathbf{r}^2 \rangle$, displays an anomalous growth with time, t , increasing as a power-law with exponent different from one, i.e., $\langle \mathbf{r}^2 \rangle \propto t^\gamma$ with $\gamma \neq 1$, as occurs in the cases of fractional Brownian motion (fBm) [2] or scaled diffusion [3].

fBm emerges when long-time correlations are present in the microscopic forces. Therefore, in isotropic media, the d -dimensional position vector $\mathbf{r} = (x_1, \dots, x_d)$ of a tracer is driven by $\dot{\mathbf{r}}(t) = \sqrt{2D} \boldsymbol{\eta}_H(t)$, where D is the diffusivity and $\boldsymbol{\eta}_H(t)$ is a vector whose components are fractional Gaussian noises with zero mean and correlations $\langle \eta_i(t) \eta_j(t + \tau) \rangle \sim \delta_{ij} \tau^{2(H-1)}$, for $\tau \neq 0$, characterized by the Hurst exponent H [2]. As a consequence, the probability distribution associated to tracers starting at the origin is given by

$$\mathcal{G}_H(\mathbf{r}, t|D) = \frac{1}{(4\pi D t^{2H})^{\frac{d}{2}}} \exp\left(-\frac{\mathbf{r}^2}{4D t^{2H}}\right), \quad (1)$$

where d is the spatial dimension. That is, the shape is Gaussian in the spatial coordinates x_i , with $i = 1, \dots, d$, which scale with time as t^H . For, $H = 1/2$, $\boldsymbol{\eta}_H(t)$ is the vector of white noise components, thus yielding normal diffusion. But, in general, for $2H \neq 1$, the diffusive spreading is Gaussian but anomalous. Experimentally, the behavior described by Eq. (1) has been observed for diverse values of H , for instance, for the diffusion of nanometric beads in crowded environments, lipid granules and telomeres, among several other cases [4–7].

However, the picture provided by Eq. (1) can change, for instance, if D depends on time and sources of heterogeneity are present, which can have a substantial impact on the statistical properties of the ensemble. A time-dependent diffusion coefficient can arise due to intrinsic or extrinsic factors, related to organisms memory and aging effects or due to transformation in the environment spatial structure [8–12]. These effects can be incorporated through scaled diffusion [3] by modulating the diffusivity with a function $\lambda(t)$.

Besides time-dependency, heterogeneity is also quite ubiquitous in real systems. Its impact can be addressed through the superstatistical approach proposed by C. Beck and E. G. D. Cohen to extend statistical mechanics to complex heterogeneous environments. Superstatistics has been applied to run-and-tumble particles [13], animal movement [14–

16], metapopulation extinction dynamics [17], time series analyses [18–21], and many other cases [22–28]. The superstatistics of fBm has been recently developed, providing theoretical support for various experimental observations, such as, protein diffusion in bacteria [29, 30], micro-particles in a bi-dimensional system with disordered distribution of pillars [31], and tracer diffusion in mucin hydrogels [32] (see Refs. [33–37] for more examples).

Throughout the next sections, we incorporate these different sources of deviation from the Bm picture and study the resulting overall probability density function (PDF),

$$p(\mathbf{r}, t) = \int_0^\infty dD \pi(D, t) \mathcal{G}_H(\mathbf{r}, t|D), \quad (2)$$

which describes the spatial distribution of the tracers, where $\mathcal{G}_H(\mathbf{r}, t|D)$ was defined in Eq. (1) and $\pi(D, t)$ is the PDF of the diffusivity D , with parameters that are function of time [38]. A similar superstatistical approach was investigated in connection with the *generalized gray Brownian process*, from the point of view of ergodicity breaking [39].

Our aim in the following sections is to obtain the reverse path, accessing the microscopic variability expressed by $\pi(D, t)$, from the macroscopic observable $p(\mathbf{r}, t)$. While the shape of the distribution (e.g., exponential, Gaussian, power-law, etc.) of diffusivities, $\pi(D, t)$, can be identified, how it spreads depends on the interplay between scaled and fractional diffusion which become blended by the superstatistical procedure, as we will see soon.

Furthermore, we explore the fact that we can reconstruct the macroscopic properties of other classes of diffusion processes, such as those embodied in the nonlinear diffusion equation, known to be generated by density-dependent feedbacks [40]. Thus, our results highlight the impact of heterogeneity and provide warnings for attempts to experimentally infer the microscopic dynamics of a given system. For particular cases, we perform numerical simulations of large heterogeneous populations, to illustrate and contextualize our analytical results.

The paper is organized as follows. In Sec. II, we present a procedure to obtain the microscopic variability from the macroscopic level, and we also provide two simple examples to illustrate the procedure. In Sec. III, we apply the theory to two general families of macroscopic distributions: stretched exponential and power-law ones. In Sec. IV, we present remarks and conclusions.

II. FROM THE MICROSCOPIC TO THE MACROSCOPIC LEVEL AND THE OTHER WAY AROUND

In this section, we first perform the superstatistical mixture, as defined by Eq. (2), obtaining the overall PDF $p(\mathbf{r}, t)$, for known microscopic variability and time-dependence of the diffusion coefficient, expressed in $\pi(D, t)$. Then, we show how to revert this process, hence allowing to extract $\pi(D, t)$ from $p(\mathbf{r}, t)$. We consider the broad scenario of self-similar

diffusion processes for which $p(\mathbf{r}, t)$ is a function of the scaled variable $\xi \equiv |\mathbf{r}|/t^{\gamma/2}$,

$$p(\mathbf{r}, t) = \frac{1}{t^{\gamma d/2}} F(|\mathbf{r}|/t^{\gamma/2}), \quad (3)$$

where the scaling function F has an arbitrary but normalizable form. Some examples are: Lévy processes [41], nonlinear diffusion [42], fractional diffusion [42, 43], among others [3, 41, 44–48] that produce non-Gaussian (lepto and platykurtic) forms.

In the current scenario, we assume that $p(\mathbf{r}, t)$ is generated by a collection of fB walkers, i.e., ruled by Eq. (1), with distinct diffusion coefficients which can change with time, $D_i = \mu_i \lambda(t)$, where μ_i , is a mobility constant and $\lambda(t)$ is, in principle, an arbitrary deterministic function that is the same for all individuals. The values of $\{\mu_i\}$ are assumed to be sampled from an unknown PDF, $\theta(\mu)$. As a consequence, in the large population limit, $N \gg 1$, diffusivity variability is well described by the PDF, $\pi(D, t) = \theta(\mu)/\lambda(t)$.

The aim of the following calculation is to uncover $\pi(D, t)$ from the ensemble PDF, $p(\mathbf{r}, t)$. To reach this result, we first apply the superstatistics recipe and then invert the procedure. As we will see, the connection between PDFs will be done through Laplace transforms, thus, it is convenient (without loss of generality) to express $\pi(D, t)$ as

$$\pi(D, t) \equiv \frac{1}{\lambda(t)} \pi_s \left(\frac{\lambda(t)}{D} \right), \quad (4)$$

where $\pi_s(y)$ is an auxiliary function that depends only on the scaled variable $y \equiv \lambda(t)/D = 1/\mu$. Substituting Eq. (4) and Eq. (1) into Eq. (2), we obtain

$$p(\mathbf{r}, t) = \int_0^\infty \frac{\bar{\pi}(y)}{(4\lambda(t) t^{2H})^{\frac{d}{2}}} \exp\left(-y \frac{\mathbf{r}^2}{4\lambda(t) t^{2H}}\right) dy, \quad (5)$$

with

$$\bar{\pi}(y) = \frac{\pi_s(y)}{\pi^{\frac{d}{2}} y^{2-\frac{d}{2}}}. \quad (6)$$

It is central to notice that the integral over y in Eq. (5) has exactly the Laplace transform structure, i.e., it has the form $\mathcal{L}_{y \rightarrow s} \{\bar{\pi}(y)\} = \int_0^\infty e^{-sy} \bar{\pi}(y) dy$, which maps y to a new variable $s = \xi^2 = \mathbf{r}^2/[4\lambda(t) t^{2H}]$.

Although there are many classes of scaled diffusion, with general time scaling $\lambda(t)$ [49, 50], self-similarity demands for a specific choice of $\lambda(t)$, to recover the scaling form of Eq. (3), then we restrict the form of $\lambda(t)$ to a power-law function of time, namely,

$$4\lambda(t) = t^{\alpha-1}. \quad (7)$$

This form embraces numerous experiments across disciplines that include the impact of aging or parameter time-dependency. For instance, physical properties of the medium, such as viscosity and temperature, can directly influence the diffusion processes and can change

over time under non-stationary constraints [12]. Also, time-dependency can be a probe to medium topology [9]. In more general settings, biological and chemical factors can be at play and influence diffusion in a complex manner (see Ref. [51] for a review).

Under the choice of $\lambda(t)$ set in Eq. (7), Eq. (5) becomes

$$p(\mathbf{r}, t) = \frac{1}{t^{(2H+\alpha-1)d/2}} \underbrace{\int_0^\infty \bar{\pi}(y) \exp\left(-y \frac{\mathbf{r}^2}{t^{2H+\alpha-1}}\right) dy}_{\mathcal{L}\{\bar{\pi}(y)\}}, \quad (8)$$

which, compared to Eq. (3), allows to identify

$$\gamma = 2H + \alpha - 1, \quad (9)$$

and

$$F(\xi) = \mathcal{L}_{y \rightarrow \xi^2} \{ \bar{\pi}(y) \}, \quad (10)$$

with $\xi = |\mathbf{r}|/t^{\gamma/2}$. That is, we can rewrite Eq. (5) in compact form as

$$p(\mathbf{r}, t) = \frac{1}{t^{\gamma d/2}} \mathcal{L}_{y \rightarrow \xi^2} \{ \bar{\pi}(y) \} \Big|_{\xi = \frac{|\mathbf{r}|}{t^{\gamma/2}}}. \quad (11)$$

First, note, from Eq. (2), that, if all the walkers have the same mobility, $\bar{D}(t)$, that is, $\pi(D, t) = \delta(D - \bar{D}(t))$, the population distribution has the Gaussian shape. Also, note that, if $\gamma \equiv 2H + \alpha - 1 = 1$, then the MSD grows linearly with time.

In fact, the μ th moment $\langle |\mathbf{r}|^\mu \rangle$ evolves according to $\langle |\mathbf{r}|^\mu \rangle \approx \mathcal{C}_{\mu,d} t^{(2H+\alpha-1)\mu/2}$ (see B), thus the growth of the second moment (i.e., $\mu = 2$) follows $\langle |\mathbf{r}|^2 \rangle \sim t^{2H+\alpha-1}$. Therefore, anomalous diffusion can be caused by correlations ruled by the exponent H , and/or time-dependency, via the exponent α . For instance, the effect of anticorrelated motion ($H < 0.5$) can be compensated by a sufficiently fast increase with time ($\alpha > 1$).

Equation (11) is the bottom-up connection providing the macroscopic-level patterns from the microscopic-level dynamics. Then, exploring Laplace-transform identifications, we can obtain a top-down connection, obtaining the micro from the macro levels, following the steps: (i) we write the overall PDF $p(\mathbf{r}, t)$ in the self-similar form (3), such that it will allow us to find the function $F(\xi) = \mathcal{L}_{y \rightarrow \xi^2} \{ \bar{\pi}(y) \}$; (ii) by means of Eq. (11), we perform the inverse Laplace transform $\mathcal{L}_{s \rightarrow y}^{-1} \{ F(\sqrt{s}) \}$ with $s = \xi^2$, to identify the $\bar{\pi}(y)$, and by using Eq. (6), we get $\pi_s(y)$; (iii) finally we arrive at $\pi(D, t)$ by means of Eq. (4)). This entire procedure is summarized by the following expression

$$\pi(D, t) = \frac{(4\pi t^{2H})^{\frac{d}{2}} t^{\alpha-1}}{4D^{2-\frac{d}{2}}} \mathcal{L}_{s \rightarrow y}^{-1} \{ p(\xi = \sqrt{s}, t) \} \Big|_{y = \frac{t^{\alpha-1}}{4D}}, \quad (12)$$

recalling that $\xi = |\mathbf{r}|/t^{(2H+\alpha-1)/2}$ and the inverse Laplace operator leads us to the change $s \xrightarrow{\mathcal{L}^{-1}} y$. For different scaling functions $F(\xi)$ in Eq. (3), different forms of $\pi(D, t)$ can emerge, such as, exponential [1, 52], χ^2 -Gamma [49, 50] and Rayleigh PDFs [53].

Importantly, we are assuming that diffusivities differ between individuals, but change deterministically over time with the same scaling factor. If the diffusivity were stochastic (producing the same $\pi(D, t)$), then, the ensemble distribution, p , would necessarily have a crossover to Gaussianity at long times, exhibiting an ensemble diffusion coefficient which is simply the average $D = N^{-1} \sum_i^N D_i$. However, for sufficiently short observation times, the superstatistical picture is present and, as a consequence, our results could be applied to this regime (for further discussion, see Refs. [1, 54]).

In the following subsections, we provide two concrete simple examples in 1D, namely, related to Laplace and nonlinear diffusion, respectively.

A. Laplace diffusion

Laplace diffusion represents a process with an exponential spread in space, which in 1D is characterized by $p(x, t) \propto \exp(-|x|/\lambda(t))$, being $\lambda(t)$ a time-dependent scaling [55, 56]. It has been reported for tracers diffusing in complex fluids, such as particles with fluctuating size [57] or hard-sphere colloidal suspensions [58], in the anomalous spreading dynamics of amoeboid cells [36], protein crowding in lipid bilayers [35], and in diffusing diffusivity models [54, 59]. There are also experiments where Laplace diffusion emerges, although only during timescales shorter than the correlation times of tracers [1, 52].

For our present purpose, let us consider a Laplace diffusion with power-law temporal scaling, given by

$$p(x, t) = \frac{1}{\sqrt{4D_0 t^\gamma}} \exp\left(-\frac{|x|}{\sqrt{D_0 t^\gamma}}\right), \quad (13)$$

in which D_0 is the ensemble diffusivity and γ a parameter that characterizes the dynamics, such that the second moment is given by $\langle x^2 \rangle = 2D_0 t^\gamma$. To uncover the superstatistics behind Eq. (13), we rewrite it in a self-similar form, in terms of the invariant variable $\xi = |x|/t^{\frac{\gamma}{2}}$, namely,

$$p(\xi, t) = \frac{1}{\sqrt{4D_0 t^\gamma}} \exp\left(-\frac{\xi}{\sqrt{D_0}}\right), \quad (14)$$

which from Eq. (9) allows us to identify $\gamma = 2H + \alpha - 1$. By substituting Eq. (14) into Eq. (12) with $d = 1$, we find the diffusivity distribution

$$\begin{aligned} \pi(D, t) &= \frac{\sqrt{\pi t^{\alpha-1}}}{4D^{\frac{3}{2}} \sqrt{D_0}} \mathcal{L}_{s \rightarrow y}^{-1} \left\{ \exp\left(-\sqrt{\frac{s}{D_0}}\right) \right\} \Big|_{y = \frac{t^{\alpha-1}}{4D}} \\ &= \frac{t^{1-\alpha}}{D_0} \exp\left(-t^{1-\alpha} \frac{D}{D_0}\right), \end{aligned} \quad (15)$$

recalling that the inversion of the Laplace transform needs to be performed on the variable $s = \xi^2$. This simple example illustrates the treatment applied to the overall PDF of tracers

to obtain the PDF of diffusivities. It is worth noting that exponential PDF of diffusivities, with time dependence, has been previously considered to analyze the ergodicity of tracer diffusion with uncorrelated noise [38].

To exercise our theoretical procedure, let us see how to obtain the diffusivity distribution from virtual experiments. We assume that single-particle tracking is not available, thus, population spreading is characterized by a population-level picture as depicted in Fig. 1. The overall PDF at time instant $t = 10$ and the temporal evolution of the MSD, associated to Laplace diffusion, are shown for different values of H and α . These parameters and diffusivity variability are in principle unknown, since we assume that individual-level information is not accessible. However, our derivations using inverse Laplace transform show that it is possible to reveal the PDF of diffusivities $\pi(D, t)$ from the shape and scaling of the MSD. In this Laplace diffusion case, the distribution is exponential but notice that, pairs (H, α) giving the same value of γ yield identical population-level results, creating ambiguity about the microscopic dynamics.

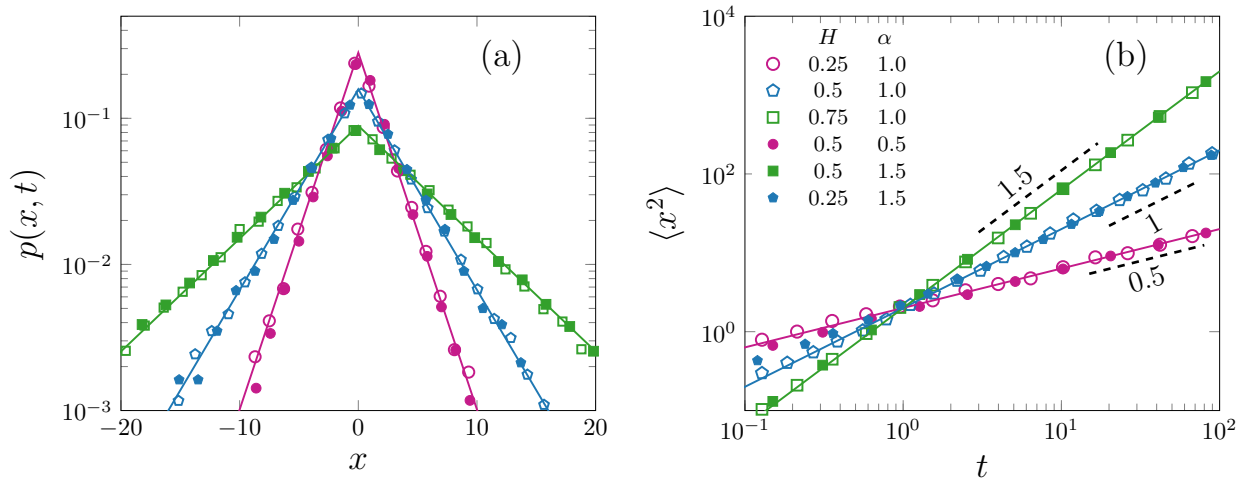


FIG. 1: **Laplace diffusion.** a) Probability density function of tracers $p(x, t)$ vs. position x , at time $t = 10$. (b) Mean square displacement $\langle x^2 \rangle$ vs. time t . Solid lines are given by Eq. (13), with $D_0 = 1$, and different values of $\gamma = 2H + \alpha - 1$. Symbols are the result of numerical simulations ($2 \cdot 10^4$ trajectories) using the corresponding values of the Hurst exponent, H , and the time scaling exponent, α (see A).

In order to explore the range of microscopic dynamics constrained by the relation $\gamma = 2H + \alpha - 1$, we perform numerical simulations of a collection of fB walker. For instance, let us consider the cases in which $\gamma = 1.5$ in Fig. 1, namely, $(H, \alpha) = (0.75, 1.0)$ and $(H, \alpha) = (0.5, 1.5)$. For both cases, a representative sample of trajectories is shown in Fig. 2. Each trajectory is independent and governed by a suitable Langevin equation, which accounts for time-dependent diffusivity and fractional noise (see A). The diffusivity of each particle is chosen from the found exponential distribution Eq. (15), with $D_0 = 1$ in all cases.

Note that despite the fact that the values of H are different (also visible in the roughness of the trajectories), diffusion time-dependency compensates its effects, resulting that, in both cases, the MSD grows with the same exponent γ . Actually, note that this ambiguity comes from the particular choice of a power-law $\lambda(t)$, needed to ensure self-similarity. Examples of underlying scenarios with static ($\alpha = 1$, empty symbols) and time-dependent ($\alpha \neq 1$, filled symbols) diffusivity are given.

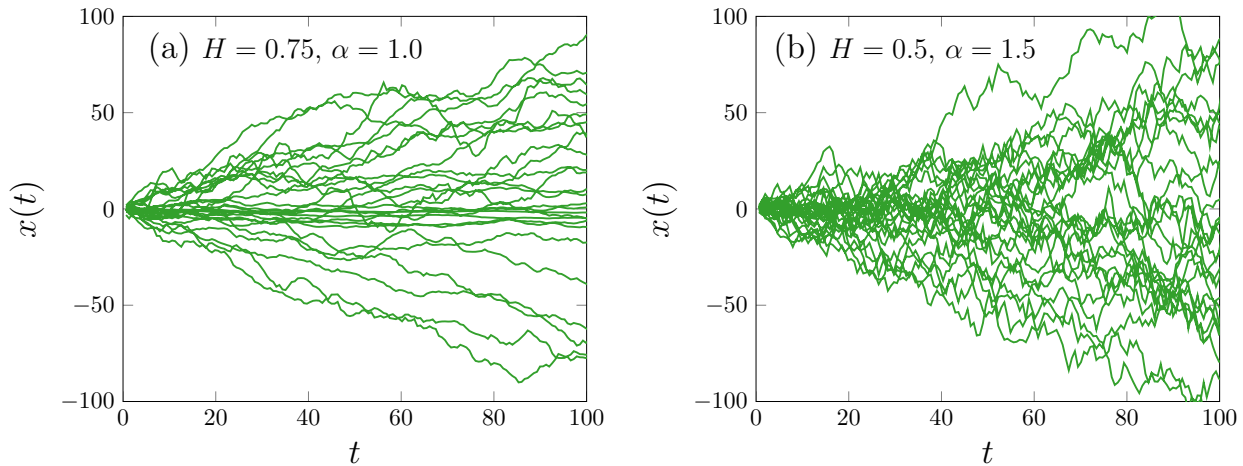


FIG. 2: Fractional Brownian walks with scaled diffusion, with the values of H and α indicated in the legends, such that $\gamma = 2H + \alpha - 1 = 1.5$. Twenty trajectories are plotted in each case. The diffusivities D were sorted according to the exponential distribution in Eq. (15) with $D_0 = 1$. Although the trajectories have visibly different nature, they lead to the same $p(x, t)$ given by Eq. (13), which characterizes Laplace diffusion.

B. Nonlinear diffusion

The nonlinear diffusion equation in 1D is defined by

$$\frac{\partial}{\partial t} p(x, t) = D_0 \frac{\partial^2}{\partial x^2} \{p(x, t)\}^m, \quad (16)$$

where D_0 is the diffusivity coefficient, and $m > -1$ is a phenomenological exponent. For $m = 1$, Eq. (16) leads to the standard diffusion equation associated to Bm. For $m \neq 1$, it phenomenologically describes the dispersion with a density-dependent diffusion coefficient that can be associated to internal feedbacks [60].

For $m > 1$, Eq. (16) is known as porous media equation [61] which implies Barenblatt-Pattle solutions, and it is associated with subdiffusion and a compact-support PDF [62, 63]. Eq. (16) can be extended to the full interval of m in which the solution is normalizable, that is, for $m > -1$, what has been theoretically considered in diverse scenarios of statistical physics [64–74]. Cases well described by $m < 1$ have been experimentally observed, in

confined granular systems [75] and in biological populations [68]. Since, we consider mixtures of Gaussian shapes (with tails that extend indefinitely), the resulting PDF of the population cannot become a compact support shape (as those yield by $m > 1$). Thus, we address only the interval $m \in (-1, 1)$, which is associated to distributions with a power-law tail, having infinite ($-1 < m < 1/3$) or finite variance ($1/3 < m < 1$), and always superdiffusive spreading $x^2 \sim t^{2/(1+m)}$.

Restricting $m \in (-1, 1]$, and using the change of exponents $m = 1 - 1/\nu$, hence $\nu \in (1/2, \infty)$, the solution of Eq. (16) can be written as

$$p(x, t) = \frac{1}{\gamma_\nu \beta_\nu t^{\frac{\nu}{2\nu-1}}} \frac{1}{\left(1 + \frac{1}{\nu \beta_\nu^2} \frac{x^2}{t^{\frac{2\nu}{2\nu-1}}}\right)^\nu}. \quad (17)$$

This normalized shape is known as q -Gaussian within the frame of nonextensive Tsallis statistics [76].

Importantly, notice that, at the same time that the exponent ν controls non-Gaussianity, it rules anomalous diffusion. The superdiffusive spreading is evident from the scaling $x^2 \sim t^{2\nu/(2\nu-1)}$ in Eq. (17), since $2\nu/(2\nu-1) > 1$ for $\nu > 1/2$. Notice that this scaling holds even when the MSD is divergent (i.e., for $1/2 < \nu < 3/2$).

The remaining coefficients in Eq. (17) are defined by $\beta_\nu = [2\nu^{-2}(\nu-1)(2\nu-1)\gamma_\nu^\frac{1}{\nu} D_0]^\frac{\nu}{2\nu-1}$ and $\gamma_\nu = \sqrt{\nu\pi} \Gamma(\frac{2\nu-1}{2})/\Gamma(\nu)$. The Gaussian shape is recovered in the limit $\nu \rightarrow \infty$, while the limit $\nu \rightarrow 1$ leads to the Cauchy-Lorentz distribution. Particularly, the Cauchy-Lorentz solution also results from the diffusion equation with μ -fractional Laplacian, taking $\mu = 1$ [77].

To show that the PDF of tracers can emerge from a mixing of fractional walkers on a disordered medium, we start by writing the solution (17) in a self-similar form, by considering $\xi = |x|/t^{\frac{\nu}{2\nu-1}}$ in Eq. (17). After comparison with Eq. (11), we obtain

$$p(\xi, t) = \frac{1}{\gamma_\nu \beta_\nu t^{(2H+\alpha-1)/2}} \frac{1}{\left(1 + \frac{\xi^2}{\nu \beta_\nu^2}\right)^\nu}, \quad (18)$$

where we have identified $2H + \alpha - 1 = \frac{2\nu}{2\nu-1}$. In this case, H and α are tangled through the exponent ν that controls both anomalous diffusion and non-Gaussianity, differently to the previous example, where they affected only the exponent of diffusive spreading γ .

To find the statistics of diffusivities, we substitute Eq. (18) into Eq. (12), leading to

$$\pi(D, t) = \frac{(4\pi t^{\alpha-1})^\frac{1}{2}}{4D^\frac{3}{2}\gamma_\nu\beta_\nu} \mathcal{L}_{s \rightarrow y}^{-1} \left\{ 1 / \left(1 + \frac{s}{\nu \beta_\nu^2}\right)^\nu \right\} \Bigg|_{y = \frac{t^{\alpha-1}}{4D}}, \quad (19)$$

with $s = \xi^2$. Performing the inverse Laplace transform in Eq. (19), we arrive at

$$\pi(D, t) = \frac{1}{\Gamma(\bar{\nu})} \frac{(\nu t^{(\alpha-1)} \beta_\nu^2 / 4)^{\bar{\nu}}}{D^{1+\bar{\nu}}} \exp\left(-\frac{\nu t^{(\alpha-1)} \beta_\nu^2}{4D}\right), \quad (20)$$

where $\bar{\nu} = \nu - 1/2 = 1/(2[2H + \alpha - 2])$ (see C). This result reveals that the superstatistics behind nonlinear diffusion gives an inverse χ^2 -Gamma distribution. Likewise in the previous section, we highlight two distinct cases: (i) for $\alpha = 1$ and hence $\gamma = 2H = 2\nu/(2\nu - 1)$, we have fractional tracers moving in a medium described by a static PDF of diffusivities; (ii) for $H = 1/2$, hence $\gamma = \alpha = 2\nu/(2\nu - 1)$, we have Brownian (non correlated) tracers moving on a medium that changes over time. Particularly, let us note that the former situation with $H = \nu/(2\nu - 1)$ was previously reported [78], although with a non-Gaussian shape generated by a stochastic process with position-dependent diffusion coefficient.

As in the Laplace diffusion case, we extract the diffusivity PDF $\pi(D, t)$ and the possible values of H and α for a given observed $\gamma = 2H + \alpha - 1$ (Eq. 20). Using this information, we performed numerical simulation of a heterogeneous collection of fB walkers. In Fig. 3, we show the population-level picture associated to nonlinear diffusion equation for different values of γ and the results obtained from the simulations for corresponding values of H and α (A).

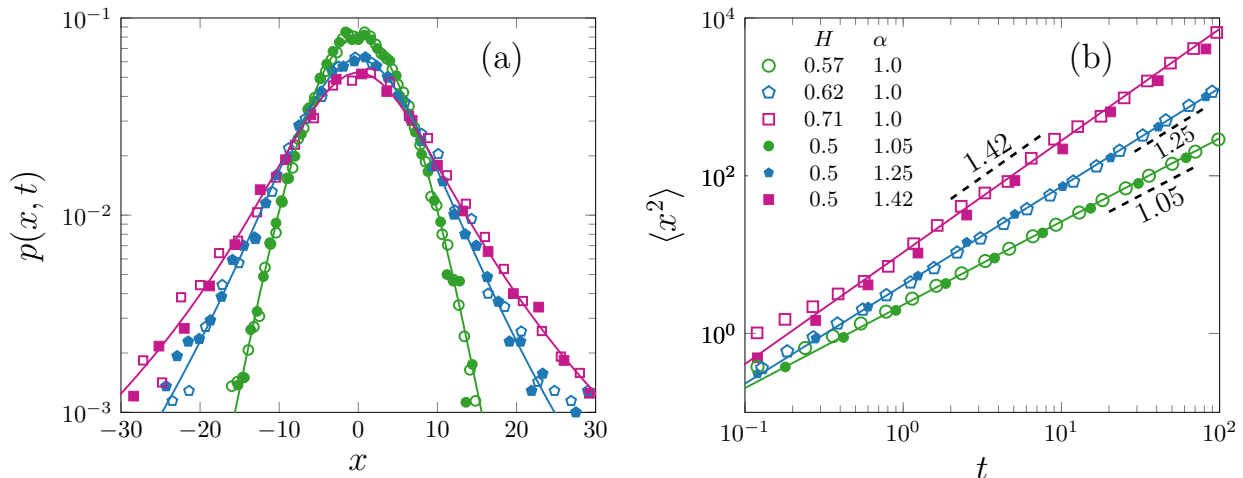


FIG. 3: **Nonlinear diffusion.** (a) Probability density function of tracers $p(x, t)$ vs. position x , at time $t = 10$. (b) Mean square displacement $\langle x^2 \rangle$ vs. time t . In both cases, we considered $D_0 = 1$ and heterogeneous tracers. Different values of exponents ν (recalling that $H = \nu/(2\nu - 1)$) and α were considered. Symbols are the result of numerical simulations ($2 \cdot 10^4$ trajectories). Solid lines are given by Eq. (20).

III. RANDOM DIFFUSIVITY OF GENERALIZED DISTRIBUTIONS

In this section, we look for the PDF of diffusivities behind generalized tracer distributions. We focus on two non-Gaussian diffusion processes that admit anomalous (or normal) diffusion. The main goal is to understand how the exponents that control the non-Gaussianity are connected to the diffusivity of the tracers.

A. Stretched diffusion

An interesting family of PDFs is the stretched exponential distribution with temporal scaling in a d -dimensional space, which is written as

$$p(\mathbf{r}, t) = \frac{1}{\mathcal{Z} (D_0 t^\gamma)^{\frac{d}{2}}} \exp\left(-\left[\frac{|\mathbf{r}|}{\sqrt{D_0 t^\gamma}}\right]^\sigma\right), \quad (21)$$

in which $\sigma \in [0, 2)$, d is the dimension number, γ control the anomalous diffusion, σ control the non-Gaussianity shape, $\mathcal{Z} = \pi^{\frac{d}{2}} \Gamma(\frac{d}{\sigma} + 1) / \Gamma(\frac{d}{2} + 1)$ and D_0 is a diffusivity-like coefficient. The stretched diffusion has been observed for particles diffusing in mucin gels [32], lateral diffusion of phospholipids and proteins [35], and large deviations of continuous time random walks [79]. For $\sigma = 1$ and $\gamma = 1$, Eq. (21) becomes reduced to the d -dimensional Laplace distribution, that was investigated in the framework of superstatistics [56]. Equation (21) can be written in self-similar form, by assuming that $\xi = |\mathbf{r}|/t^{\gamma/2}$, yielding

$$p(\xi, t) = \frac{1}{\mathcal{Z} (D_0 t^{2H+\alpha-1})^{\frac{d}{2}}} \exp\left(-\left[\frac{\xi}{\sqrt{D_0}}\right]^\sigma\right) \quad (22)$$

where $\gamma = 2H + \alpha - 1$. Applying the Eq. (22) into (12) with $0 < \sigma < 2$, we find the follow PDF for diffusivity

$$\begin{aligned} \pi(D, t) &= \frac{(4\pi)^{\frac{d}{2}} t^{(\alpha-1)(1-\frac{d}{2})}}{4D_0^{\frac{d}{2}} \mathcal{Z} D^{2-\frac{d}{2}}} \mathcal{L}_{s \rightarrow y}^{-1} \left\{ \exp\left(-\frac{s^{\frac{\sigma}{2}}}{D_0^{\frac{\sigma}{2}}}\right) \right\} \Bigg|_{y = \frac{t^{\alpha-1}}{4D}} \\ &= \frac{\pi^{\frac{d}{2}} t^{(\alpha-1)(1-\frac{d}{2})}}{4^{1-\frac{d}{2}} D_0^{\frac{d}{2}-1} \mathcal{Z} D^{2-\frac{d}{2}}} L_{\sigma/2} \left(\frac{D_0 t^{\alpha-1}}{4D} \right), \end{aligned} \quad (23)$$

where $L_{\sigma/2}(z)$ is the one-sided Lévy function. For $\sigma \rightarrow 1$ we have $L_{1/2}(z) = \frac{1}{2\sqrt{\pi z^{\frac{3}{2}}}} \exp\left(-\frac{1}{4z}\right)$ that implies a χ^2 -Gamma distribution of diffusivities

$$\pi(D, t) = \frac{4^{\frac{d}{2}} \pi^{\frac{d-1}{2}} t^{-(\alpha-1)(\frac{1+d}{2})}}{\mathcal{Z} D_0^{\frac{d+1}{2}} D^{\frac{1-d}{2}}} \exp\left(-t^{1-\alpha} \frac{D}{D_0}\right), \quad (24)$$

recalling that $\mathcal{Z} = \pi^{\frac{d}{2}} \Gamma(\frac{d}{\sigma} + 1) / \Gamma(\frac{d}{2} + 1)$. Special cases of Eq. (24) that has been investigated before include: $\sigma = 1$, $\alpha = 1$ and $H = 1/2$ for d -dimensional Laplace diffusion [56]; $\sigma = 1$ and $d = 1$ for uncorrelated noise [38]. For $\sigma \neq 1$, the PDF (23) is a new result within the superstatistics of random walks.

B. Power-law diffusion

We consider an overall PDF of tracers that has a power-law tail, similarly to the solution of the nonlinear diffusion equation. Then, we suggest the generalized PDF

$$p(\mathbf{r}, t) = \frac{1}{\mathcal{Z} (\beta t^\gamma)^{\frac{d}{2}}} \frac{1}{\left(1 + \frac{\mathbf{r}^2}{\beta t^\gamma}\right)^\nu}, \quad (25)$$

where $\gamma \in [0, 2]$ and $\nu \in (1/d, \infty)$ are independent parameters, and $\mathcal{Z} = (\pi)^{\frac{d}{2}} \Gamma(|\nu| - \frac{d}{2}) / \Gamma(|\nu|)$ allows to satisfy $\int_0^\infty S_d r^{d-1} p(\mathbf{r}, t) dr = 1$ with $S_d = d\pi^{d/2} / \Gamma(\frac{d}{2} + 1)$. Here, the γ and ν control anomalous diffusion and non-Gaussianity, respectively. Then, the nonlinear diffusion solution is a particular case where γ is coupled to ν . The PDF distribution of tracers (25) has numerous applications in complex systems, for example in modeling of protein diffusion within bacteria [29], parliamentary presence data [80] and stock markets [81].

To reveal the PDF of diffusivities embodied in power-law diffusion, we identify $\xi = |x|/t^{\gamma/2}$ in Eq. (25), which allows us to write the self-similar form

$$p(\xi, t) = \frac{1}{\mathcal{Z} (\beta t^{2H+\alpha-1})^{\frac{d}{2}}} \frac{1}{\left(1 + \frac{\xi^2}{\beta}\right)^\nu}, \quad (26)$$

where, as before, we identified $\gamma = 2H + \alpha - 1$. Now, applying this self-similar solution in Eq. (12) for the d -dimensional case, we have that the random diffusivity obeys the PDF

$$\pi(D, t) = \frac{1}{\mathcal{Z} (\beta t^\gamma)^{\frac{d}{2}}} \frac{(4\pi t^{2H})^{\frac{d}{2}} t^{\alpha-1}}{4D^{2-\frac{d}{2}}} \mathcal{L}_{s \rightarrow \xi}^{-1} \left\{ 1 / \left(1 + \frac{s}{\beta}\right)^\nu \right\} \Bigg|_{y = \frac{t^{\alpha-1}}{4D}}, \quad (27)$$

where $\xi = \sqrt{s}$. Performing the inverse Laplace transform, we have

$$\pi(D, t) = \frac{(\beta t^{\alpha-1}/4)^{\nu-\frac{d}{2}}}{D^{\nu-\frac{d}{2}+1} \Gamma(\nu - d/2)} \exp\left(-t^{\alpha-1} \frac{\beta}{4D}\right), \quad (28)$$

where $\nu > d/2$. The χ^2 -Gamma distribution of the inverse diffusivity arises in Eq. (28), regardless of the fractional features of the walker. Moreover, large diffusivity fluctuations, i.e., $\pi(D) \propto D^{-\nu-1+d/2}$ with $\alpha = 1$, imply a different route to a similar asymptotic limit reported within the framework of Lévy flights [82].

IV. DISCUSSIONS AND FINAL REMARKS

Random diffusivity (or mobility) has been reported in a range of experimental settings and can be associated to different (intrinsic and extrinsic) sources. From the theoretical point of view, the impact of such variability can be addressed through the superstatistics formalism, which brings forth interesting insights of how individual tracers diffusion may produce complex population-level properties.

In this paper, we presented a procedure to compute the PDF of diffusivities from an overall PDF of tracers that is self-similar. Our procedure considers the mixing of fractional Brownian walkers with a PDF of diffusivities that may change over time following a power-law time scaling. This approach includes different sources of anomalous diffusion, namely, diffusivities that change over time ($\alpha \neq 1$) or fractional dynamics ($H \neq 1/2$), or both. Thus,

we connected a broad class of possible population density distributions to their corresponding variability in the diffusion coefficient.

Well-known cases, such as Laplace diffusion and nonlinear diffusion, were investigated and used to exemplify the application of our general results. More complex cases were addressed subsequently, reaching a vast range of scenarios observed experimentally, including fat-tailed and stretched-exponential distributions. The generality of our results allowed us to see how certain classes of diffusion processes are interpreted in terms of diffusivity variability. For instance, we found that nonlinear-diffusion behavior is achieved when the parameters γ and ν (which characterize the scaling of the MSD and the shape of the distribution, respectively) are not independent, namely, they are related through $\frac{2\nu}{2\nu-1} = \gamma = 2H + \alpha - 1$, implying that, in the distribution of the diffusivity, given by the inverse χ^2 -Gamma Eq. (20), both the fractional exponent H , and also the scaling exponent α , participate in an entangled way. It is worth to recall that the nonlinear diffusion is assumed to be driven by $\partial_t p = \nabla^2(p^m)$, which embodies a density-dependent feedback [40], while, the spread of heterogeneous fBws (which is state-independent) can produce the same macroscopic features.

Despite the existing interference in the connection between individual-level mobility and the population PDF, using a proper setting and with additional knowledge about the system, experimental approaches could benefit from our results. For that, it would be necessary to record the spread of a given population with sufficient temporal and spatial resolution to extract the scaling of the MSD (parameter γ) and to estimate the shape of the distribution (function F). The shape should be resolved under the scaled representation, $\xi = |\mathbf{r}|/t^{\frac{\gamma}{2}}$, which is assumed to be preserved during the spread. Then, performing numerically (or, when possible, analytically) the inverse Laplace transform in Eq. (12), the distribution of diffusivities, $\pi(D)$, can be obtained. This is the procedure we followed, from a theoretical perspective, for paradigmatic diffusion pictures (Figs. 1 and 3).

We highlight the fact that the overall MSD of tracers carries ambiguity about the source of anomalous diffusion, i.e., $\langle \mathbf{r}^2 \rangle \propto t^\gamma$ with $\gamma = 2H + \alpha - 1$, being indistinguishable which interpretation leads to the anomalous diffusion exponent. To know precisely what is the anomalous diffusion mechanism, complementary information about tracer's trajectories (Fig. 2) and environment spatiotemporal structure need to be provided.

Future research should focus on keep extending the connection between diffusivity variability and population distribution. First, if the population PDF, $p(\mathbf{r}, t)$, were separable as $p(\mathbf{r}, t) = F(\xi)/[g(t)]^d$, with $\xi = |\mathbf{r}|/g(t)$, where $g(t)$ can be an arbitrary function (not necessarily a power-law in time), then, our approach based on the Laplace transform formalism could still be used, extending the scope of applicability beyond the addressed self-similar scenario. In the current case, we have considered $g(t) \propto \lambda(t)t^{2H}$ with $\lambda(t) \propto t^{\alpha-1}$. But, if the walkers were not of a fB type, or if diffusion time-dependency $\lambda(t)$ were not a power-law, then, the ambiguity about their contributions in spreading might be broken. As a consequence, one could infer more information about the microscopic dynamics. This discussion suggests natural extensions worth of future investigation, for instance, the one in which

$\lambda(t) \propto e^{\pm\lambda_0 t}$ [12].

Another step forward would be to address the mixing of diffusion process with short or long tails, such as q -Gaussian [76] with $q < 1$ (finite support) and $q > 1$ (power-law tails), respectively, that by itself introduce a connection between the shape of the population distribution and the scaling of the MSD. Finally, it would be also interesting to explore other forms of heterogeneity, e.g., in the α exponent of the scaling $\lambda(t) \propto t^{\alpha-1}$ or in the Hurst exponent H [29], which in our case are the same for all the walkers.

Acknowledgments: CA acknowledges Brazilian agency CNPq (process 311435/2020-3) for partial financial support. MAFS and CA acknowledge CAPES (finance code 001).

Appendix A: Microscopic dynamics

In individual-level simulations, we generate the trajectories of each fB walker $i = 1, 2, \dots, N$ from microscopic rules. The fractional component is related to the Hurst exponent H , and each individual is associated to a different diffusion coefficient, $D_i(t) = \mu_i \lambda(t)$, where μ_i is a mobility constant in time but different for each walker, and λ is the deterministic protocol, common to all walkers. The heterogeneity of the ensemble is given by sampling the values of μ_i from a probability distribution $\theta(\mu)$ at the beginning of our simulations.

Then, the microscopic dynamics of each walker is evolved through a Langevin-like equation that incorporates fractional motion and time scaling, as

$$\dot{x} = \sqrt{2\mathcal{D}(t)}\eta_H(t), \quad (\text{A1})$$

where $\mathcal{D}(t) = \mu\alpha t^{\alpha-1}/4$ [38] and η_H is the fractional noise with Hurst exponent H [2], generated by using the so-called Davies–Harte algorithm [83].

Appendix B: Anomalous diffusion

The general μ -moment, according to the superstatistical mixture of fB walkers defined in Eq. (2), is given by

$$\langle |\mathbf{r}|^\mu \rangle = \int_0^\infty \int_{|\mathbf{r}|} |\mathbf{r}|^\mu \frac{4}{\lambda(t)} \pi_s \left(\frac{\lambda}{D} \right) \mathcal{G}_H(\mathbf{r}, t|D) |\mathbf{r}|^{d-1} S_d d\mathbf{r} dD \quad (\text{B1})$$

where $S_d = d\pi^{d/2}/\Gamma(\frac{d}{2} + 1)$. Performing the following calculations

$$\begin{aligned} \langle |\mathbf{r}|^\mu \rangle &= \int_0^\infty \int_{|\mathbf{r}|} \frac{|\mathbf{r}|^\mu}{(4t^{2H}\pi D)^{\frac{d}{2}}} \exp\left(-\frac{\mathbf{r}^2}{4t^{2H}D}\right) \frac{\pi_s(\lambda(t)/D)}{\lambda(t)} |\mathbf{r}|^{d-1} S_d d\mathbf{r} dD \\ &= \int_0^\infty \frac{\pi_s(\lambda(t)/D)}{\lambda(t)} \int_{|\mathbf{r}|} \frac{|\mathbf{r}|^\mu}{(4t^{2H}\pi D)^{\frac{d}{2}}} \exp\left(-\frac{\mathbf{r}^2}{4t^{2H}D}\right) |\mathbf{r}|^{d-1} S_d d\mathbf{r} dD \\ &= t^{H\mu} \int_0^\infty \frac{\pi_s(\lambda(t)/D)}{\lambda(t)} \frac{d2^{\mu-1} D^{\frac{\mu}{2}} \Gamma\left(\frac{d+\mu}{2}\right)}{\Gamma\left(\frac{d}{2} + 1\right)} dD \end{aligned} \quad (\text{B2})$$

and redefining a new integration variable $\bar{r} = |\mathbf{r}/t^H|$, Eq. (B2) implies

$$\langle |\mathbf{r}|^\mu \rangle = t^{H\mu} (\lambda(t))^{\frac{\mu}{2}} \frac{2^{\mu-1} dD^{\frac{\mu}{2}} \Gamma\left(\frac{d+\mu}{2}\right)}{\Gamma\left(\frac{d}{2} + 1\right)} \int_0^\infty \pi_s(y) y^{-2-\frac{\mu}{2}} dy. \quad (\text{B3})$$

Assuming the power-law temporal behavior for $\lambda(t) \sim t^{\alpha-1}$, as argued in the main text, we obtain

$$\langle |\mathbf{r}|^\mu \rangle \sim t^{(2H+\alpha-1)\frac{\mu}{2}}, \quad (\text{B4})$$

as presented in Sec II.

Appendix C: PDF of diffusivities for nonlinear diffusion

Starting from Eq. (19), presented in Sec. IIB, our goal is to use the equation

$$\pi(D, t) = \frac{(4\pi t^{\alpha-1})^{\frac{1}{2}}}{4D^{\frac{3}{2}} \gamma_\nu \beta_\nu} \mathcal{L}^{-1} \left\{ \left(1 + \frac{\xi}{\nu \beta_\nu^2} \right)^{-\nu} \right\} \Bigg|_{y = \frac{t^{\alpha-1}}{4D}} \quad (\text{C1})$$

to find Eq. (20). Using the Laplace inverse transform, we have

$$\begin{aligned} \pi(D, t) &= \frac{(4\pi t^{\alpha-1})^{\frac{1}{2}}}{4D^{\frac{3}{2}} \gamma_\nu \beta_\nu} \left[y^{\nu-1} (\nu \beta_\nu^2)^\nu \frac{\exp(-y \nu \beta_\nu^2)}{\Gamma(\nu)} \right] \Bigg|_{y = \frac{t^{\alpha-1}}{4D}} \\ &= \frac{\nu^\nu \sqrt{4\pi t^{\alpha-1}}}{4\sqrt{D^3} \gamma_\nu \beta_\nu^{1-2\nu}} \left[y^{\nu-1} \frac{\exp(-y \nu \beta_\nu^2)}{\Gamma(\nu)} \right] \Bigg|_{y = \frac{t^{\alpha-1}}{4D}} \end{aligned} \quad (\text{C2})$$

that implies

$$\pi(D, t) = \frac{(\nu \beta_\nu^2/4)^{\nu-\frac{1}{2}} t^{(\alpha-1)(\nu-1/2)}}{D^{(\nu-1/2)+1} \Gamma(\nu - \frac{1}{2})} \exp\left(-\frac{\nu \beta_\nu^2 t^{(\alpha-1)}}{4D}\right). \quad (\text{C3})$$

Defining a new parameter $\bar{\nu} = \nu - 1/2$, we write the inverse χ^2 -Gamma distribution with time dependence

$$\pi(D, t) = \frac{1}{\Gamma(\bar{\nu})} \frac{(\nu t^{(\alpha-1)} \beta_\nu^2/4)^{\bar{\nu}}}{D^{1+\bar{\nu}}} \exp\left(-\frac{\nu t^{(\alpha-1)} \beta_\nu^2}{4D}\right), \quad (\text{C4})$$

as shown in Eq. (20).

[1] B. Wang, S. M. Anthony, S. C. Bae, S. Granick, Anomalous yet Brownian, Proceedings of the National Academy of Sciences 106 (36) (2009) 15160–15164.

- [2] B. B. Mandelbrot, J. W. Van Ness, Fractional Brownian motions, fractional noises and applications, *SIAM Review* 10 (4) (1968) 422–437.
- [3] S. Lim, S. Muniandy, Self-similar Gaussian processes for modeling anomalous diffusion, *Physical Review E* 66 (2) (2002) 021114.
- [4] D. Ernst, M. Hellmann, J. Köhler, M. Weiss, Fractional Brownian motion in crowded fluids, *Soft Matter* 8 (18) (2012) 4886–4889.
- [5] J.-H. Jeon, V. Tejedor, S. Burov, E. Barkai, C. Selhuber-Unkel, K. Berg-Sørensen, L. Oddershede, R. Metzler, In vivo anomalous diffusion and weak ergodicity breaking of lipid granules, *Physical Review Letters* 106 (4) (2011) 048103.
- [6] E. Kepten, I. Bronshtein, Y. Garini, Ergodicity convergence test suggests telomere motion obeys fractional dynamics, *Physical Review E* 83 (2011) 041919.
- [7] K. Burnecki, E. Kepten, J. Janczura, I. Bronshtein, Y. Garini, A. Weron, Universal algorithm for identification of fractional Brownian motion. A case of telomere subdiffusion, *Biophysical Journal* 103 (9) (2012) 1839–1847.
- [8] L. L. Latour, K. Svoboda, P. P. Mitra, C. H. Sotak, Time-dependent diffusion of water in a biological model system, *Proceedings of the National Academy of Sciences* 91 (4) (1994) 1229–1233.
- [9] P. N. Sen, Time-dependent diffusion coefficient as a probe of geometry, *Concepts in Magnetic Resonance Part A: An Educational Journal* 23 (1) (2004) 1–21.
- [10] H. Safdari, A. V. Chechkin, G. R. Jafari, R. Metzler, Aging scaled Brownian motion, *Physical Review E* 91 (4) (2015) 042107.
- [11] D. S. Novikov, E. Fieremans, S. N. Jespersen, V. G. Kiselev, Quantifying brain microstructure with diffusion MRI: Theory and parameter estimation, *NMR in Biomedicine* 32 (4) (2019) e3998.
- [12] A. G. Cherstvy, H. Safdari, R. Metzler, Anomalous diffusion, nonergodicity, and ageing for exponentially and logarithmically time-dependent diffusivity: striking differences for massive versus massless particles, *Journal of Physics D: Applied Physics* 54 (19) (2021) 195401.
- [13] F. J. Sevilla, A. V. Arzola, E. P. Cital, Stationary superstatistics distributions of trapped run-and-tumble particles, *Physical Review E* 99 (1) (2019) 012145.
- [14] S. Petrovskii, A. Morozov, Dispersal in a statistically structured population: fat tails revisited, *The American Naturalist* 173 (2) (2009) 278–289.
- [15] S. Hapca, J. W. Crawford, I. M. Young, Anomalous diffusion of heterogeneous populations characterized by normal diffusion at the individual level, *Journal of the Royal Society Interface* 6 (30) (2009) 111–122.
- [16] J. Santana-Filho, E. Raposo, A. Macêdo, G. Vasconcelos, G. Viswanathan, F. Bartumeus, M. da Luz, A Langevin dynamics approach to the distribution of animal move lengths, *Journal of Statistical Mechanics: Theory and Experiment* 2020 (2) (2020) 023406.
- [17] E. H. Colombo, Connecting metapopulation heterogeneity to aggregated lifetime statistics,

- Ecological Complexity 39 (2019) 100777.
- [18] C. Beck, E. G. Cohen, H. L. Swinney, From time series to superstatistics, *Physical Review E* 72 (5) (2005) 056133.
 - [19] R. Mendes, L. Malacarne, C. Anteneodo, Statistics of football dynamics, *The European Physical Journal B* 57 (3) (2007) 357–363.
 - [20] A. Cortines, R. Riera, C. Anteneodo, Measurable inhomogeneities in stock trading volume flow, *EPL (Europhysics Letters)* 83 (3) (2008) 30003.
 - [21] C. Anteneodo, S. D. Queirós, Statistical mixing and aggregation in Feller diffusion, *Journal of Statistical Mechanics: Theory and Experiment* 2009 (10) (2009) P10023.
 - [22] V. García-Morales, K. Krischer, Superstatistics in nanoscale electrochemical systems, *Proceedings of the National Academy of Sciences* 108 (49) (2011) 19535–19539.
 - [23] M. Hidalgo-Soria, E. Barkai, S. Burov, Cusp of non-Gaussian density of particles for a diffusing diffusivity model, *Entropy* 23 (2) (2021) 231.
 - [24] M. A. F. dos Santos, I. S. Gomez, B. G. da Costa, O. Mustafa, Probability density correlation for PDM-Hamiltonians and superstatistical PDM-partition functions, *The European Physical Journal Plus* 136 (1) (2021) 1–18.
 - [25] H. Agahi, M. Khalili, Truncated Mittag-Leffler distribution and superstatistics, *Physica A: Statistical Mechanics and its Applications* 555 (2020) 124620.
 - [26] M. A. F. dos Santos, Mittag-Leffler functions in superstatistics, *Chaos, Solitons & Fractals* 131 (2020) 109484.
 - [27] M. A. F. dos Santos, L. Menon Junior, Log-Normal Superstatistics for Brownian Particles in a Heterogeneous Environment, *Physics* 2 (4) (2020) 571–586.
 - [28] A. J. Rominger, M. A. Fuentes, P. A. Marquet, Nonequilibrium evolution of volatility in origination and extinction explains fat-tailed fluctuations in Phanerozoic biodiversity, *Science Advances* 5 (6) (2019) 0122.
 - [29] C. Beck, Y. Itto, Superstatistical modelling of protein diffusion dynamics in bacteria, *Journal of the Royal Society Interface* .
 - [30] A. A. Sadoon, Y. Wang, Anomalous, non-Gaussian, viscoelastic, and age-dependent dynamics of histonelike nucleoid-structuring proteins in live *Escherichia coli*, *Physical Review E* 98 (4) (2018) 042411.
 - [31] I. Chakraborty, Y. Roichman, Disorder-induced Fickian, yet non-Gaussian diffusion in heterogeneous media, *Physical Review Research* 2 (2) (2020) 022020.
 - [32] A. G. Cherstvy, S. Thapa, C. E. Wagner, R. Metzler, Non-Gaussian, non-ergodic, and non-Fickian diffusion of tracers in mucin hydrogels, *Soft Matter* 15 (12) (2019) 2526–2551.
 - [33] A. Sabri, X. Xu, D. Krapf, M. Weiss, Elucidating the origin of heterogeneous anomalous diffusion in the cytoplasm of mammalian cells, *Physical Review Letters* 125 (5) (2020) 058101.
 - [34] P.-Y. Gires, M. Thampi, M. Weiss, Quantifying active diffusion in an agitated fluid, *Physical Chemistry Chemical Physics* 22 (38) (2020) 21678–21684.

- [35] J.-H. Jeon, M. Javanainen, H. Martinez-Seara, R. Metzler, I. Vattulainen, Protein crowding in lipid bilayers gives rise to non-Gaussian anomalous lateral diffusion of phospholipids and proteins, *Physical Review X* 6 (2) (2016) 021006.
- [36] A. G. Cherstvy, O. Nagel, C. Beta, R. Metzler, Non-Gaussianity, population heterogeneity, and transient superdiffusion in the spreading dynamics of amoeboid cells, *Physical Chemistry Chemical Physics* 20 (35) (2018) 23034–23054.
- [37] T. J. Lampo, S. Stylianidou, M. P. Backlund, P. A. Wiggins, A. J. Spakowitz, Cytoplasmic RNA-protein particles exhibit non-Gaussian subdiffusive behavior, *Biophysical Journal* 112 (3) (2017) 532–542.
- [38] X. Wang, Y. Chen, Ergodic property of Langevin systems with superstatistical, uncorrelated or correlated diffusivity, *Physica A: Statistical Mechanics and its Applications* (2021) 126090.
- [39] D. Molina-García, T. M. Pham, P. Paradisi, C. Manzo, G. Pagnini, Fractional kinetics emerging from ergodicity breaking in random media, *Physical Review E* 94 (5) (2016) 052147.
- [40] E. H. Colombo, C. Anteneodo, Nonlinear population dynamics in a bounded habitat, *Journal of Theoretical Biology* 446 (2018) 11–18.
- [41] V. V. Uchaikin, Self-similar anomalous diffusion and Lévy-stable laws, *Physics-Uspekhi* 46 (8) (2003) 821.
- [42] M. Bologna, C. Tsallis, P. Grigolini, Anomalous diffusion associated with nonlinear fractional derivative Fokker-Planck-like equation: Exact time-dependent solutions, *Physical Review E* 62 (2) (2000) 2213.
- [43] G. Pagnini, Erdélyi-Kober fractional diffusion, *Fractional calculus and applied analysis* 15 (1) (2012) 117–127.
- [44] V. V. Uchaikin, Subordinated Lévy–Feldheim motion as a model of anomalous self-similar diffusion, *Physica A: Statistical Mechanics and its Applications* 305 (1-2) (2002) 205–208.
- [45] R. Ferrari, A. Manfroi, W. Young, Strongly and weakly self-similar diffusion, *Physica D: Nonlinear Phenomena* 154 (1-2) (2001) 111–137.
- [46] F. A. Oliveira, R. Ferreira, L. C. Lapas, M. H. Vainstein, Anomalous diffusion: A basic mechanism for the evolution of inhomogeneous systems, *Frontiers in Physics* 7 (2019) 18.
- [47] M. A. F. dos Santos, Analytic approaches of the anomalous diffusion: A review, *Chaos, Solitons & Fractals* 124 (2019) 86–96.
- [48] F. Mainardi, G. Pagnini, R. Saxena, Fox H functions in fractional diffusion, *Journal of Computational and Applied Mathematics* 178 (1-2) (2005) 321–331.
- [49] V. Sposini, A. V. Chechkin, F. Seno, G. Pagnini, R. Metzler, Random diffusivity from stochastic equations: comparison of two models for Brownian yet non-Gaussian diffusion, *New Journal of Physics* 20 (4) (2018) 043044.
- [50] M. A. F. dos Santos, L. M. Junior, Random diffusivity models for scaled Brownian motion, *Chaos, Solitons & Fractals* 144 (2021) 110634.
- [51] G. Muñoz-Gil, G. Volpe, M. A. García-March, R. Metzler, M. Lewenstein, C. Manzo, The

- Anomalous Diffusion challenge: objective comparison of methods to decode anomalous diffusion 11804.
- [52] B. Wang, J. Kuo, S. C. Bae, S. Granick, When Brownian diffusion is not Gaussian, *Nature materials* 11 (6) (2012) 481–485.
 - [53] A. G. Cherstvy, R. Metzler, Anomalous diffusion in time-fluctuating non-stationary diffusivity landscapes, *Physical Chemistry Chemical Physics* 18 (34) (2016) 23840–23852.
 - [54] A. V. Chechkin, F. Seno, R. Metzler, I. M. Sokolov, Brownian yet non-Gaussian diffusion: from superstatistics to subordination of diffusing diffusivities, *Physical Review X* 7 (2) (2017) 021002.
 - [55] R. Metzler, Superstatistics and non-Gaussian diffusion, *The European Physical Journal Special Topics* 229 (5) (2020) 711–728.
 - [56] E. Postnikov, A. Chechkin, I. Sokolov, Brownian yet non-Gaussian diffusion in heterogeneous media: from superstatistics to homogenization, *New Journal of Physics* 22 (6) (2020) 063046.
 - [57] M. Hidalgo-Soria, E. Barkai, Hitchhiker model for Laplace diffusion processes, *Physical Review E* 102 (1) (2020) 012109.
 - [58] J. Guan, B. Wang, S. Granick, Even hard-sphere colloidal suspensions display Fickian yet non-Gaussian diffusion, *ACS nano* 8 (4) (2014) 3331–3336.
 - [59] M. V. Chubynsky, G. W. Slater, Diffusing diffusivity: a model for anomalous, yet Brownian, diffusion, *Physical Review Letters* 113 (9) (2014) 098302.
 - [60] V. Dornelas, E. H. Colombo, C. Anteneodo, Single-species fragmentation: The role of density-dependent feedback, *Physical Review E* 99 (6) (2019) 062225.
 - [61] L. A. Peletier, The porous media equation, *Applications of nonlinear analysis in the physical sciences* 6 (1981) 229–241.
 - [62] M. Muskat, The flow of homogeneous fluids through porous media, *Soil Science* 46 (2) (1938) 169.
 - [63] P. I. Polubarinova-Koch, *Theory of ground water movement*, Princeton University Press, 2015.
 - [64] T. D. Frank, *Nonlinear Fokker-Planck equations: fundamentals and applications*, Springer Science & Business Media, 2005.
 - [65] S. Abe, C. Beck, E. G. Cohen, Superstatistics, thermodynamics, and fluctuations, *Physical Review E* 76 (3) (2007) 031102.
 - [66] A. Plastino, A. Plastino, Non-extensive statistical mechanics and generalized Fokker-Planck equation, *Physica A: Statistical Mechanics and its Applications* 222 (1-4) (1995) 347–354.
 - [67] C. Tsallis, D. J. Bukman, Anomalous diffusion in the presence of external forces: Exact time-dependent solutions and their thermostistical basis, *Physical Review E* 54 (3) (1996) R2197.
 - [68] G. Mendes, M. Ribeiro, R. Mendes, E. Lenzi, F. Nobre, Nonlinear Kramers equation associated with nonextensive statistical mechanics, *Physical Review E* 91 (5) (2015) 052106.
 - [69] C. Anteneodo, Non-extensive random walks, *Physica A: Statistical Mechanics and its Appli-*

- cations 358 (2-4) (2005) 289–298.
- [70] V. Schwämmle, F. D. Nobre, C. Tsallis, q -Gaussians in the porous-medium equation: stability and time, *The European Physical Journal B* 66 (4) (2008) 537–546.
- [71] N. M. Mutothya, Y. Xu, Y. Li, R. Metzler, Characterising stochastic motion in heterogeneous media driven by coloured non-Gaussian noise, *Journal of Physics A: Mathematical and Theoretical* .
- [72] L. Santos, Microscopic dynamics of nonlinear Fokker-Planck equations, *Physical Review E* 103 (3) (2021) 032106.
- [73] E. Gravanis, E. Akylas, G. Livadiotis, Stochastic dynamics and superstatistics of the many-particle kappa distribution, *Journal of Statistical Mechanics: Theory and Experiment* 2021 (5) (2021) 053201.
- [74] A. I. Lavrova, E. B. Postnikov, Barenblatt-like approach to transport processes in meningeal lymphatic vessel’s dynamics, *The European Physical Journal Plus* 136 (5) (2021) 1–9.
- [75] G. Combe, V. Richefeu, M. Stasiak, A. P. Atman, Experimental validation of a nonextensive scaling law in confined granular media, *Physical Review Letters* 115 (23) (2015) 238301.
- [76] C. Tsallis, *Introduction to nonextensive statistical mechanics: approaching a complex world*, Springer Science & Business Media, 2009.
- [77] R. Metzler, J. Klafter, The random walk’s guide to anomalous diffusion: a fractional dynamics approach, *Physics Reports* 339 (1) (2000) 1–77.
- [78] L. Borland, Microscopic dynamics of the nonlinear Fokker-Planck equation: A phenomenological model, *Physical Review E* 57 (6) (1998) 6634.
- [79] W. Wang, E. Barkai, S. Burov, Large deviations for continuous time random walks, *Entropy* 22 (6) (2020) 697.
- [80] D. S. Vieira, J. M. Riveros, M. Jauregui, R. S. Mendes, Anomalous diffusion behavior in parliamentary presence, *Physical Review E* 99 (4) (2019) 042141.
- [81] F. Alonso-Marroquin, K. Arias-Calluari, M. Harré, M. N. Najafi, H. J. Herrmann, q -Gaussian diffusion in stock markets, *Physical Review E* 99 (6) (2019) 062313.
- [82] R. Jain, K. Sebastian, Lévy flight with absorption: a model for diffusing diffusivity with long tails, *Physical Review E* 95 (3) (2017) 032135.
- [83] R. B. Davies, D. Harte, Tests for Hurst effect, *Biometrika* 74 (1) (1987) 95–101.